

This is a repository copy of *Diagnostic Method for Photovoltaic Systems based on Six Layer Detection Algorithm*.

White Rose Research Online URL for this paper:

<https://eprints.whiterose.ac.uk/177684/>

Version: Accepted Version

Article:

Dhimish, Mahmoud, Holmes, Violeta, Mehrdadi, Bruce et al. (1 more author) (2017) Diagnostic Method for Photovoltaic Systems based on Six Layer Detection Algorithm. *Electric Power Systems Research*. pp. 26-39.

<https://doi.org/10.1016/j.epsr.2017.05.024>

Reuse

Items deposited in White Rose Research Online are protected by copyright, with all rights reserved unless indicated otherwise. They may be downloaded and/or printed for private study, or other acts as permitted by national copyright laws. The publisher or other rights holders may allow further reproduction and re-use of the full text version. This is indicated by the licence information on the White Rose Research Online record for the item.

Takedown

If you consider content in White Rose Research Online to be in breach of UK law, please notify us by emailing eprints@whiterose.ac.uk including the URL of the record and the reason for the withdrawal request.

Diagnostic Method for Photovoltaic Systems Based on Six Layer Detection Algorithm

Mahmoud Dhimish, Violeta Holmes, Bruce Mehrdadi, Mark Dales

Department of Computing and Engineering, University of Huddersfield, Huddersfield, United Kingdom

Abstract

This work proposes a fault detection algorithm based on the analysis of the theoretical curves which describe the behaviour of an existing grid-connected photovoltaic (GCPV) plant. For a given set of working conditions, solar irradiance and PV modules' temperature, a number of attributes such as voltage ratio (VR) and power ratio (PR) are simulated using virtual instrumentation (VI) LabVIEW software. Furthermore, a third order polynomial function is used to generate two detection limits (high and low limit) for the VR and PR ratios obtained using LabVIEW simulation tool.

The high and low detection limits are compared with real-time long-term data measurements from a 1.1kWp and 0.52kWp GCPV systems installed at the University of Huddersfield, United Kingdom. Furthermore, samples that lies out of the detecting limits are processed by a fuzzy logic classification system which consists of two inputs (VR and PR) and one output membership function.

The obtained results show that the fault detection algorithm can accurately detect different faults occurring in the PV system. The maximum detection accuracy of the algorithm before considering the fuzzy logic system is equal to 95.27%, however, the fault detection accuracy is increased up to a minimum value of 98.8% after considering the fuzzy logic system.

Keywords: *Photovoltaic System, Photovoltaic Faults, Fault Detection, LabVIEW, Fuzzy Logic*

1. INTRODUCTION

Despite the fact that Grid-Connected Photo-Voltaic (GCPV) systems have no moving parts, and therefore usually require low maintenance, they are still subject to various failures and faults associated with the PV arrays, batteries, power conditioning units, utility interconnections and wiring [1-2]. It is especially difficult to shut down PV modules completely during faulty conditions related to PV arrays (DC side) [3]. It is therefore required to create algorithms to facilitate the detection of possible faults occurring in GCPV installations [4].

There are existing fault detection techniques for use in GCPV plants. Some use satellite data for fault prediction as presented by M. Tadj et al [5], this approach is based on satellite image for estimating solar radiation data and predicting faults occurring in the DC side of the GCPV plant. However, some algorithms do not require any climate data, such as solar irradiance and modules' temperature, but instead use earth capacitance measurements in a technique established by Taka-Shima et al [6].

Some fault detection methods use an automatic supervision based on the analysis of the output power for the GCPV system. A. Chouder & S. Silvestre et al [7], presented a new automatic supervision and fault detection technique which use a standard divination method ($\pm 2\sigma$) for detecting various faults in PV

39 systems such as faulty modules in a PV string and faulty maximum power point tracking (MPPT) units.
40 However, S. Silverstre et al [8] presented a new fault detection algorithm based on the evaluation of the
41 current and output voltage indicators for analyzing the type of fault occurred in PV systems installations.

42 A photovoltaic fault detection technique based on artificial neural network (ANN) is proposed by W.
43 Chine et al [9]. The technique is based on the analysis of the voltage, power and the number of peaks in
44 the current-voltage (I-V) curve characteristics. However, [10-11], proposed a fault detection algorithm
45 which allows the detection of seven different fault modes on the DC-side of the GCPV system. The
46 algorithm uses the t-test statistical analysis technique for identifying the presence of systems fault
47 conditions.

48 Other fault detection algorithms focus on faults occurring on the AC-side of GCPV systems, as proposed
49 by R. Platon et al [12]. The approach uses $\pm 3\sigma$ statistical analysis technique for identifying the faulty
50 conditions in the DC/AC inverter units. Moreover, hot-spot detection in PV substrings using the AC
51 parameters characterization was developed by [13]. The hot-spot detection method can be further used
52 and integrated with DC/DC power converters that operates at the subpanel level. Nevertheless, the
53 analysis of the current and voltage indicators in a GCPV system operating in partial shading faulty
54 conditions is created by Silvestre et al [14].

55 A comprehensive review of the faults, trends and challenges of the grid-connected PV systems is
56 explained by M. Obi & R. bass, M. Alam et al and A. khamis et al [15-17].

57 Currently, fuzzy logic systems widely used with GCPV plants. R. Boukenoui et al [18] proposed a new
58 intelligent MPPT method for standalone PV system operating under fast transient variations based on
59 fuzzy logic controller (FLC) with scanning and storing algorithm. Furthermore, [19] presents an adaptive
60 FLC design technique for PV inverters using differential search algorithm. However, to the best of our
61 knowledge, few of the reviewed articles used a fuzzy classifier system in order to investigate the faulty
62 condition occurring in the DC-side of the GCPV system.

63 Since many fault detection algorithms use statistical analysis techniques such as [7, 10, 11 and 12], this
64 work proposes a fault detection algorithm that does not depend on any statistical approaches in order to
65 classify faulty conditions in PV systems. Furthermore, some existing fault detection techniques such as
66 [20-21] use a complex power circuit design to facilitate the fault detection in GCPV plants. However, the
67 proposed fault detection algorithm depends only on the variations of the voltage and the power, which
68 makes the algorithm simple to construct and reused in wide range of GCPV plants.

69 In this work, we present the development of a fault detection algorithm which allows the detection of
70 possible faults occurring on the DC-side of GCPV systems. The algorithm is based on the analysis of
71 theoretical voltage ratio (VR) and power ratio (PR) for the examined GCPV plant. High and low detection
72 limits are generated using 3rd order polynomial functions which are obtained using the simulated data of
73 the VR and PR ratios. Subsequently, if the theoretical curves are not capable to detect the type of the fault
74 occurred in the GCPV system, a fuzzy logic classifier system is designed to facilitate the fault type
75 detecting for the examined PV system. A software tool is designed using Virtual Instrumentation (VI)
76 LabVIEW software to automatically display and monitor the possible faults occurring within the GCPV
77 plant. A LabVIEW VI is also used to log the measured power, voltage and current data for the entire
78 GCPV system, more details regarding the VI LabVIEW structure is presented in [22].

79 The main contribution of this work is the development and the theoretical implementation of a simple,
80 fast and reliable GCPV fault detection algorithm. The algorithm does not depend on any statistical
81 techniques which makes it easier to facilitate and detect faults based on theoretical curves analysis and

82 fuzzy logic classification system. In practice, the proposed fault detection algorithm is capable of
 83 localizing and identifying faults occurring on the DC-side of GCPV systems. The types of fault which can
 84 be detected are based on the size of the GCPV plant, which will be discussed in the next section. The
 85 algorithm is based on a six layer method working sequentially as shown in Fig. 1.

86 This paper is organized as follows: Section 2 describes the methodology used which includes the PV
 87 theoretical power curve modelling and the proposed fault detection algorithm, while section 3 explains
 88 the validation and a brief discussion of the proposed fault detection algorithm. Finally, section 4 describes
 89 the conclusion and future work.

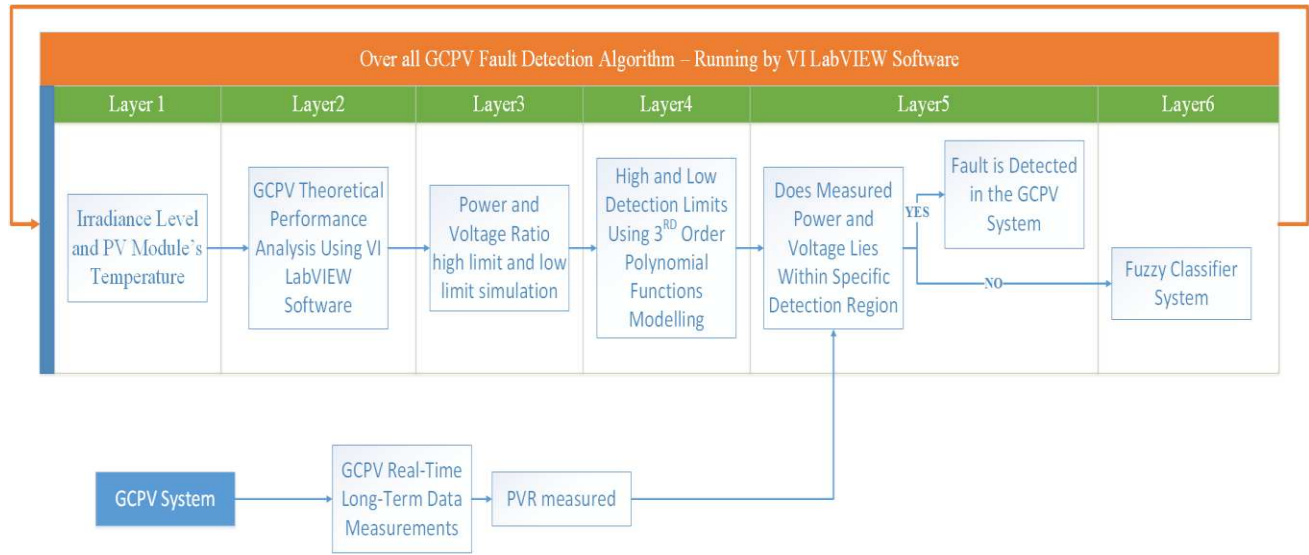


Fig. 1. Over all GCPV fault detection algorithm Layers

90 2. METHODOLOGY

91 2.1 Photovoltaic Theoretical Power Curve Modelling

92 The DC side of the GCPV system is modelled using the 5-parameter model. The voltage and current
 93 characteristics of the PV module can be obtained using the single diode model [23] as follows:

$$94 \quad I = I_{ph} - I_o \left(e^{\frac{V+IR_s}{nsV_t}} - 1 \right) - \frac{V+IR_s}{R_{sh}} \quad (1)$$

95 Where I_{ph} is the photo-generated current at STC, I_o is the dark saturation current at STC, R_s is the
 96 module series resistance, R_{sh} is the panel parallel resistance, ns is the number of series cells in the PV
 97 module and V_t is the thermal voltage and it can be defined based on:

$$98 \quad V_t = \frac{AKT}{q} \quad (2)$$

99 Where A the ideal diode factor, k is Boltzmann's constant and q is the charge of the electron.

100 The five parameter model is determined by solving the transcendental equation (1) using Newton-
 101 Raphson algorithm [24] based only on the datasheet of the available parameters for the examined PV
 102 module that was used in this work as shown in Table 1. The power produced by the PV module in watts
 103 can be easily calculated along with the current (I) and voltage (V) that is generated by equation (1),
 104 therefore:

105
$$P_{\text{theoretical}} = I \times V \tag{3}$$

106 The Power-Voltage (P-V) curve analysis of the tested PV module is shown in Fig. 2. The maximum
 107 power and voltage for each irradiance level under the same temperature value can be expressed by the P-
 108 V curves.

109 The purpose of using the analysis for the P-V curves, is to generate the expected output power of the
 110 examined PV module, therefore, it can be used to predict the error between the measured PV data and the
 111 theoretical power and voltage performance.

112 The proposed PV fault detection algorithm can detect various fault in the GCPV plants such as:

- 113 • Partial shading (PS) condition effects the GCPV system
- 114 • 1 Faulty PV module and PS
- 115 • 2 Faulty PV modules and PS
- 116 • 3 Faulty PV modules and PS
- 117 ○
- 118 ○
- 119 ○
- 120 • (n-1) Faulty PV modules and PS, where m is the total number of PV modules in the GCPV
- 121 installation.

122 A briefly explanation of the proposed fault detection algorithm is presented in section 2.2 and section 2.3.

TABLE 1
 ELECTRICAL CHARACTERISTICS OF SMT6 (60) P PV MODULE

Solar Panel Electrical Characteristics	Value
Peak Power	220 W
Voltage at maximum power point (V_{mp})	28.7 V
Current at maximum power point (I_{mp})	7.67 A
Open Circuit Voltage (V_{oc})	36.74 V
Short Circuit Current (I_{sc})	8.24 A
Number of cells connected in series	60
Number of cells connected in parallel	1
R_s, R_{sh}	0.48 Ohms , 258.7 Ohms
dark saturation current (I_o)	2.8×10^{-10} A
Ideal diode factor (A)	1.5
Boltzmann's constant (K)	1.3806×10^{-23} J.K ⁻¹

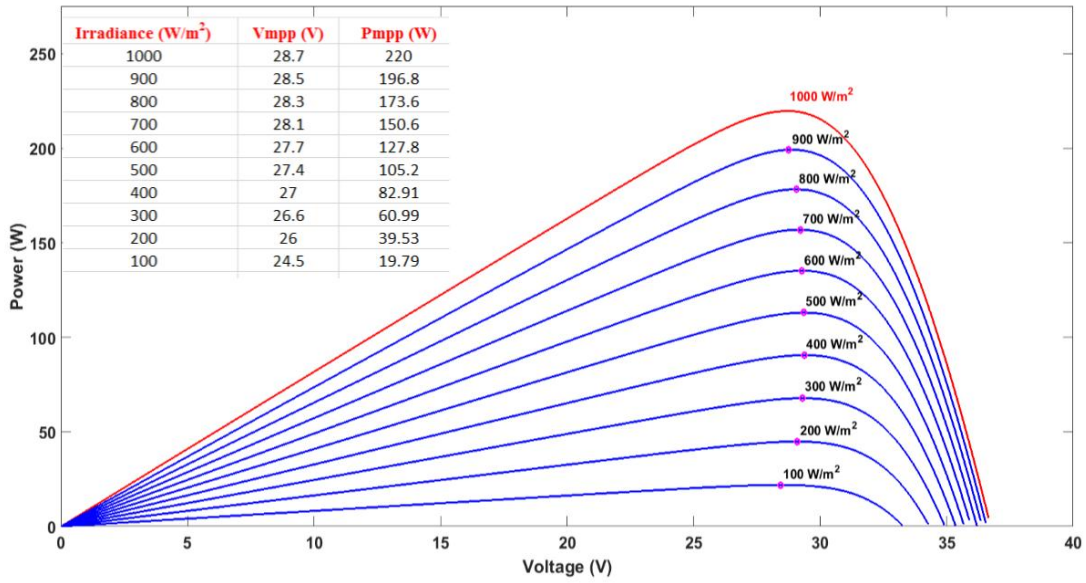


Fig. 2. Power-Voltage (P-V) curve modelling under various irradiance levels

2.2 Proposed Fault Detection Algorithm: Theoretical Curves Modelling

123 The main objective of the fault detection algorithm is to detect and determine when and where a fault has
 124 occurred in the GCPV plant.

125 The first layer of the fault detection algorithm passes the measured irradiance level and photovoltaic
 126 module's temperature to VI LabVIEW software in order to generate the expected theoretical P-V curve as
 127 described previously in section 2.1. This layer is shown in Fig. 3.

128 To determine if a fault has occurred in a GCPV system, two ratios have been identified. The theoretical
 129 Power ratio (PR) and the theoretical voltage ratio (VR) have been used to categorize the region of the
 130 fault. It is necessary to use both ratios because:

- 131 1. Both ratios are changeable during faulty conditions in the PV systems
- 132 2. When the power ratio is equal to zero, the voltage ratio can still have a value regarding the
 133 voltage open circuit of the PV modules

134 The power and voltage ratios are given by the following expressions:

$$135 \quad PR = \frac{P_{G,T}}{P_{G,T} - nP_0} \quad (4)$$

$$136 \quad VR = \frac{V_{G,T}}{V_{G,T} - nV_0} \quad (5)$$

137 Where $P_{G,T}$ is the theoretical output power generated by the GCPV system at specific G (irradiance) and
 138 T (module temperature) values, n is the number of PV modules, $V_{G,T}$ is the theoretical output voltage
 139 generated by the GCPV system at specific G (irradiance) and T (module temperature) values and both
 140 V_0 , P_0 are the maximum operating voltage and power at STC (G: 1000 w/m², T: 25 °C) respectively.

141 The number of faulty PV modules can be expressed by the number of PV modules in the examined PV
 142 string. For example, if the PV string comprises 5 photovoltaic modules connected in series, then, $n = 5$.

143 In reality, the internal sensors used to measure the voltage and current for a GCPV system have
 144 efficiencies of less than 100%. This tolerance rate must therefore be considered in the PR and VR ratio
 145 calculations. For this instance, the PR and VR values are divided into two limits:

- 146 1. High limit: where the maximum operating efficiency of the sensors is applied, therefore, the high
 147 limit for both PR and VR ratios is expressed by (4) and (5).
- 148 2. Low limit: where the efficiency (tolerance rate) of the sensors is applied. Both limits can be
 149 expressed by the following formulas:

$$150 \quad PR \text{ Low limit} = \frac{P_{G,T}}{(P_{G,T} - nP_0)\eta_{sensor}} \quad (6)$$

$$151 \quad VR \text{ Low limit} = \frac{V_{G,T}}{(V_{G,T} - nV_0)\eta_{sensor1}} \quad (7)$$

152 Where η_{sensor} is the efficiency of both the voltage and current sensor, while, $\eta_{sensor1}$ is the efficiency of
 153 the voltage sensor:

$$154 \quad \eta_{sensor} = \eta_{sensor1}(\text{Voltage Sensor efficiency}) + \eta_{sensor2}(\text{Current Sensor efficiency}) \quad (8)$$

155 The PR and VR high and low detection limits are evaluated for the examined GCPV system using various
 156 irradiance levels, as described in the third layer in Fig. 3. For this particular layer, the analysis of the PR
 157 vs. VR curves can be seen in the example shown next to layer 5, Fig. 3. This example shows the high and
 158 low detection limit for two case scenarios: one faulty PV module and two faulty PV modules, where both
 159 curves are created using 3rd order polynomial functions. The purpose of the 3rd order polynomial curves is
 160 to generate a regression function which describes the performance of the curves which are created by the
 161 theoretical points using VI LabVIEW software.

162 The overall GCPV fault detecting algorithm is explained in Fig. 3. Layer 5, shows the measured data vs.
 163 the 3rd order polynomial curves generated by VI LabVIEW software. The measured PR and measured VR
 164 can be evaluated using the following formula:

$$165 \quad \text{Measured PR vs. Measured VR} = \frac{P_{G,T}}{P_{MEASURED}} \text{ vs. } \frac{V_{G,T}}{V_{MEASURED}} \quad (9)$$

166 In case of which the measured PR vs. VR is out of range:

$$167 \quad F \text{ High limit} < \text{Measured PR vs. Measured VR} < F \text{ low limit}$$

168 Therefore, the fault detection algorithm cannot identify the type of the fault that has occurred in the
 169 GCPV plant. However, it can predict two possible faulty conditions which might have occurred in the
 170 GCPV system. As shown in Fig. 3, layer 5 example. The measured data 2 indicates two possible faulty
 171 conditions:

- 172 1. Faulty PV module and partial shading effects on the GCPV system
- 173 2. Two faulty PV modules and partial shading effects on the GCPV system

174 Therefore, out of region samples is processed by a fuzzy logic classifier as shown in Fig 3, layer 6.

175 The difference between the proposed theoretical curve modelling with other similar approaches described
 176 by [7, 8, 9, 10 and 14] is that the algorithm contains the number of modules in the GCPV system, also the
 177 approach is using 3rd order polynomial function which can be used to plot a regression function that
 178 describes the behavior of the faulty region and the design of a fuzzy logic fault classification which is
 179 described in the next section (section 2.3).

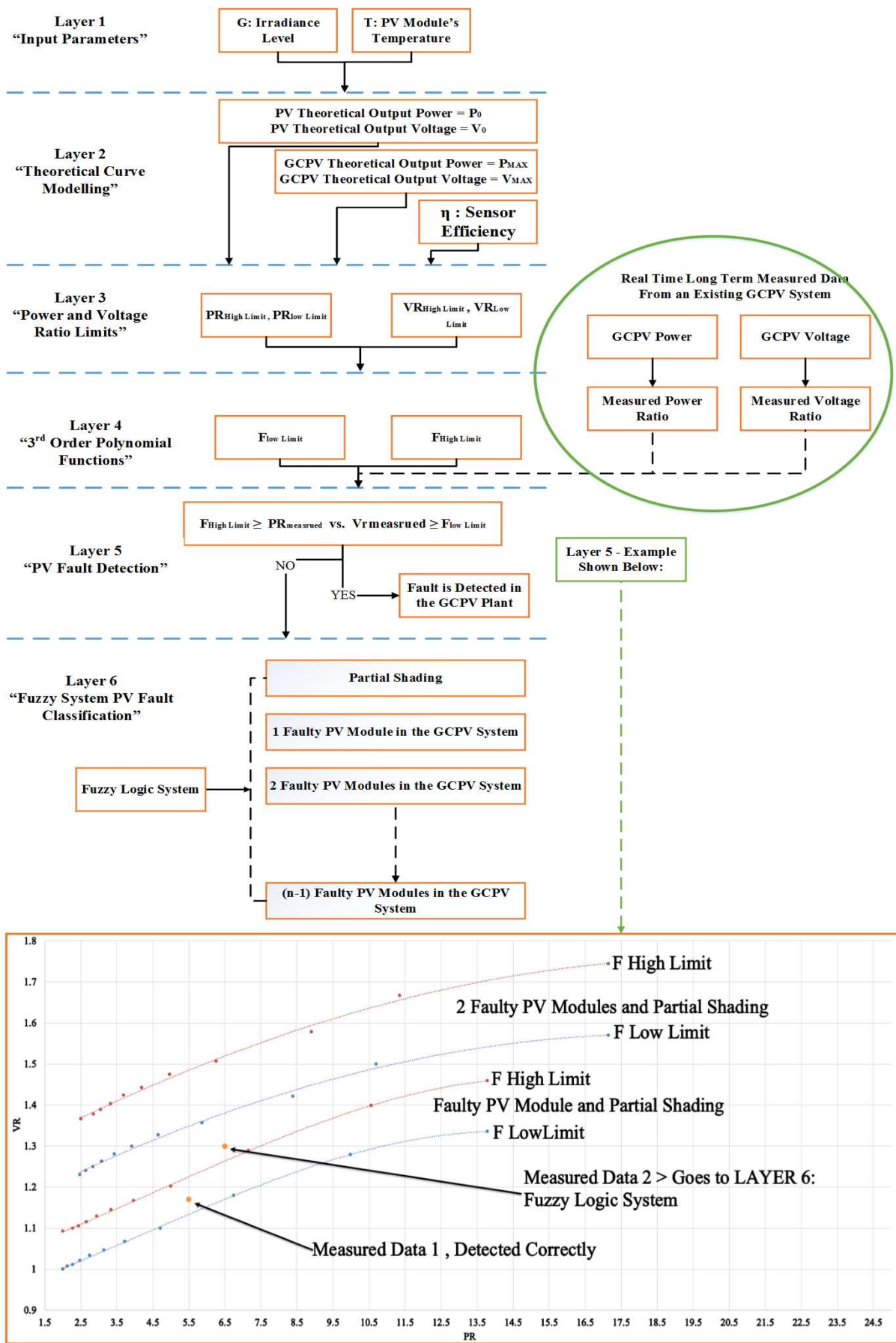


Fig. 3. Detailed flowchart for the proposed fault detection algorithm which contains 5 layers

2.3 Proposed Fault Detection Algorithm: Fuzzy Logic Classifier

181 Nowadays, fuzzy logic systems became more in use with PV systems. A brief overview of the recent
 182 publications on fuzzy logic system design is presented by L. Suganthi [25]. From the literature reviewed
 183 previously in the introduction, currently, there are a lack of research in the field of fuzzy logic
 184 classification systems which are used in examining faulty conditions in PV plants. Therefore, in this
 185 paper, a fuzzy logic classifier is demonstrated and verified experimentally.

186 Fig. 4 describes the overall fuzzy logic classifier system design. The fuzzy logic system consists of two
 187 inputs: voltage ratio (VR) and the power ratio (PR), denoted in Fig. 4 as (A) and (B) respectively. The
 188 membership function for each input is divided into five fuzzy sets described as: PS (partial shading
 189 condition), 1 (one faulty PV module), 2 (two faulty PV modules), 3 (three faulty PV modules) and 4 (four
 190 faulty PV modules). The fuzzy interface applies the approach of Mamdani method (min-max) managed
 191 by the fuzzy logic system rule, stage 2 of the fuzzy logic system. After the rules application, the output is
 192 applied to classify the fault detection type occurred in the GCPV plant.

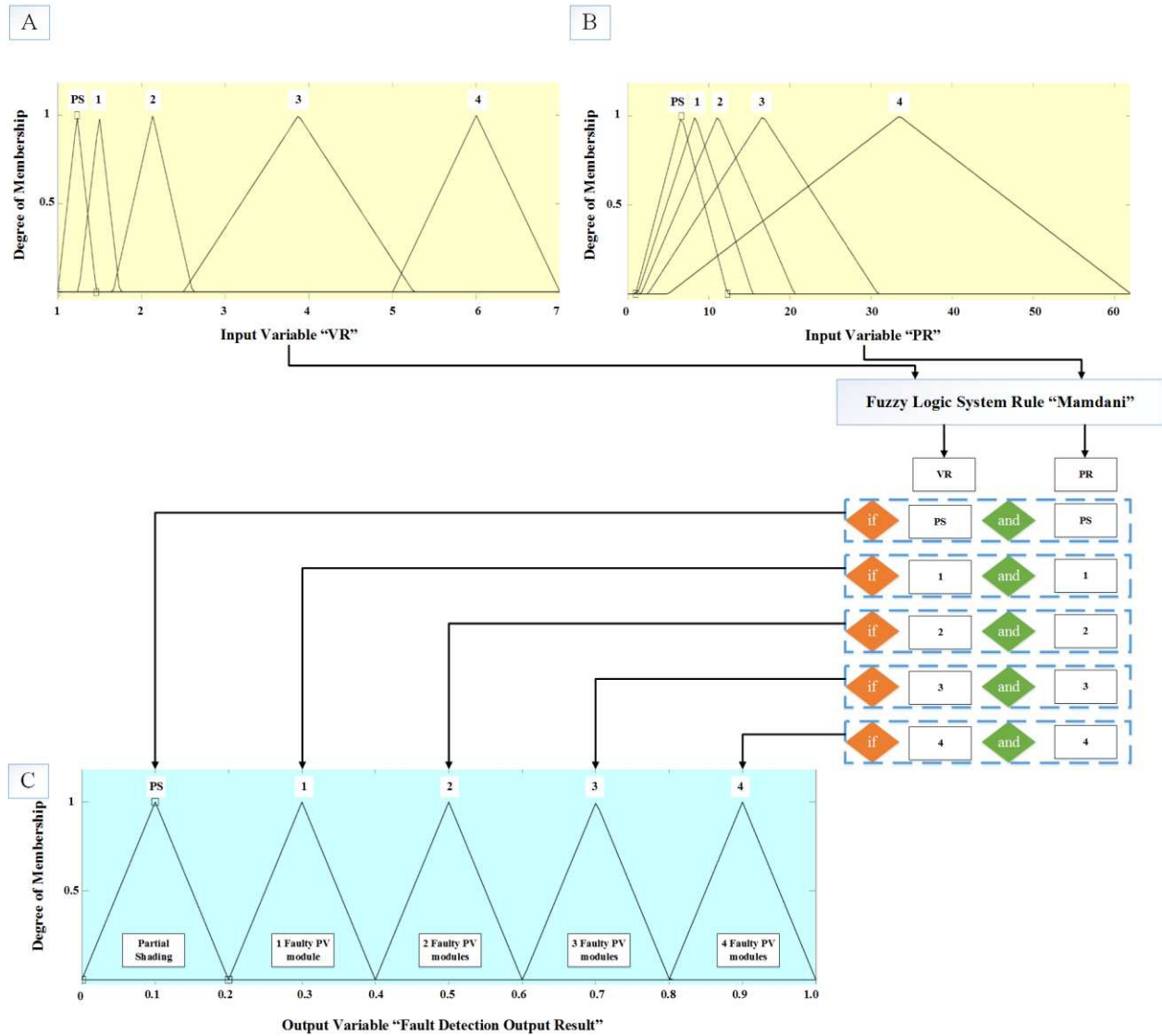


Fig. 4. Fuzzy Logic classifier system design. (A) Voltage ratio input, (B) Power ratio input, (C) Fault detection output

193 A brief calculation of each membership function for VR, PR and the fuzzy logic membership output
 194 function is reported in Fig. 5. The membership functions are based on the mathematical calculation of the
 195 examined GCPV plant used in this work. The examined GCPV system which is used to evaluate the
 196 performance of the fault detection algorithm is demonstrated briefly in section 3.1: experimental setup.
 197 Both fuzzy logic system inputs VR and PR are evaluated at the maximum power and voltage of the
 198 GCPV system which are equal to 1100Wp and 143.5V. In addition, the mathematical calculations
 199 includes the PS conditions which might affect the performance of the entire PV system.

200 The fuzzy logic system rule are based on: if, and statement. Each case scenario is presented after the
 201 fuzzy logic system rule shown in Fig. 4(C). However, the output membership function is divided into 5
 202 sets: PS (0 - 0.2), faulty PV module (0.2 – 0.4), two faulty PV modules (0.4 – 0.6), three faulty PV
 203 modules (0.6 – 0.8) and four faulty PV modules (0.8 – 1.0).

204 Furthermore, the output surface for the fuzzy logic classifier system is plotted and represented by a 3D
 205 fitting curve shown in Fig. 6. Where the x-axis presents the PR, y-axis presents VR and the fault detection
 206 output classification is on the z-axis.

207 In order to generalize the proposed fuzzy logic classification systems, it is required to input the values of
 208 the voltage and the power to the fuzzy interface system, and then, the faulty region could be calculated
 209 using the formulas (4 & 5) for the variations of the power and voltage respectively. Additionally, the
 210 output detection membership function could be extended up to the value of the PV modules connected in
 211 series in each PV string separately and this extension in the membership function can be evaluated within
 212 the region of 0 to 1 as the following: 1/ number of series PV modules in the PV string.

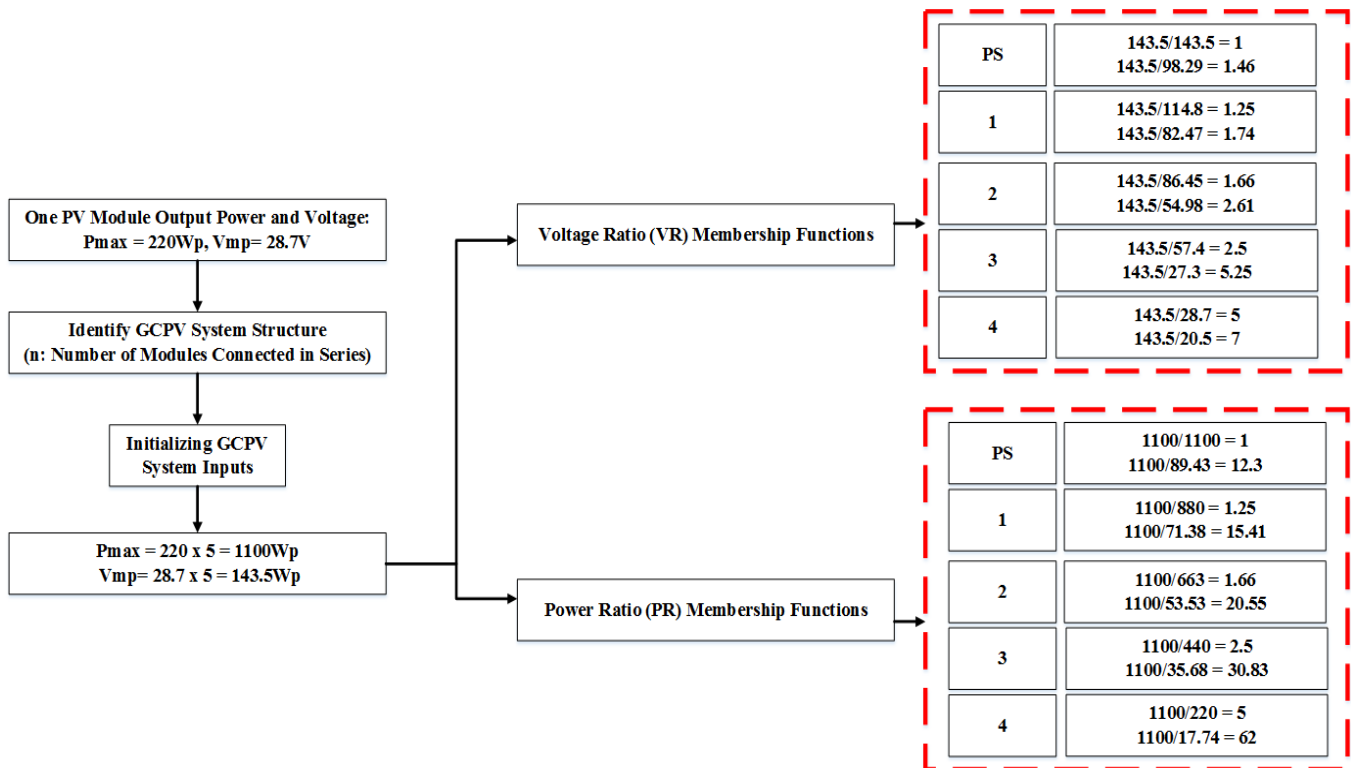


Fig. 5. Mathematical calculations for the fuzzy logic classifier system including VR, PR, Rules and Output Membership Function

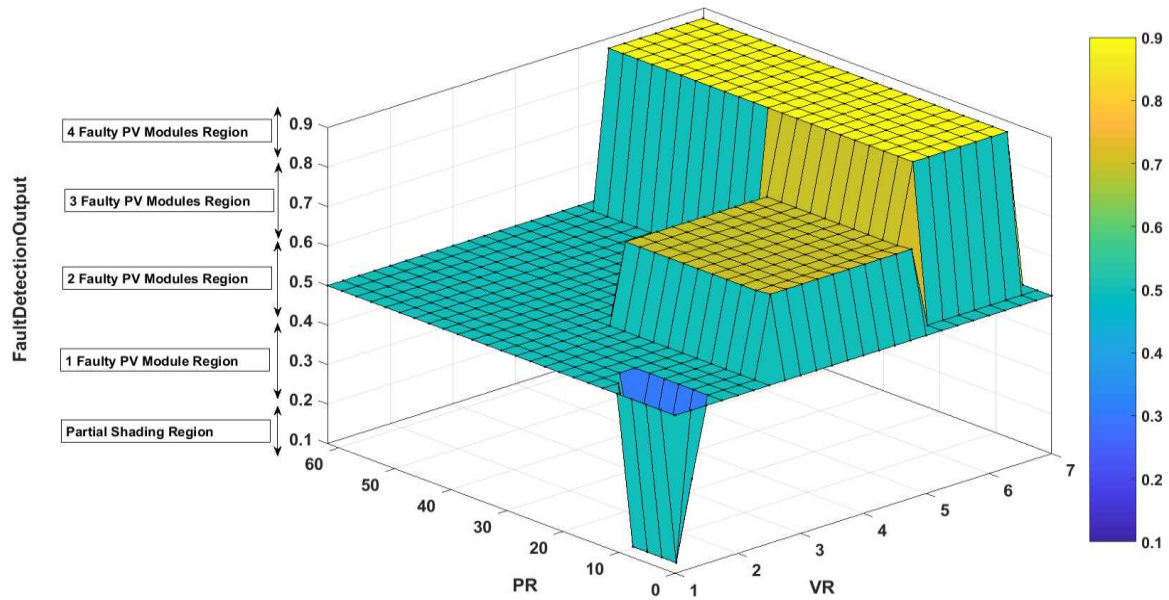


Fig. 6. Fuzzy Logic classifier output surface with VR, PR and the fault detection output membership function

213 3. *GCPV Fault Detection Algorithm Validation*

214 In this section, the performance of the proposed fault detection algorithm is verified. For this purpose, the
 215 acquired data for various days have been considered using 1.1kWp grid-connected PV plant. The time
 216 zone for all measurements is GMT.

217 3.1 *Experimental Setup*

218 The PV system used in this work consists of a grid-connected PV plant comprising 5 polycrystalline
 219 silicon PV modules each with a nominal power of 220 Wp. The photovoltaic modules are connected in
 220 series. The photovoltaic string is connected to a Maximum Power Point Tracker (MPPT) with an output
 221 efficiency of not less than 95.0%. The DC current and voltage are measured using the internal sensors
 222 which are part of the FLEXmax MPPT unit. A battery bank is used to store the energy produced by the
 223 PV plant.

224 A Vantage Pro monitoring unit is used to receive the Global solar irradiance measured by the Davis
 225 weather station which includes a pyranometer. A Hub 4 communication manager is used to facilitate
 226 acquisition of modules' temperature using the Davis external temperature sensor, and the electrical data
 227 for each photovoltaic string. VI LabVIEW software is used to implement data logging and monitoring
 228 functions of the GCPV system. Fig. 7 illustrates the overall system architecture of the GCPV plant.

229 The real-time measurements are taken by averaging 60 samples, gathered at a rate of 1Hz over a period of
 230 one minute. Therefore, the obtained results for power, voltage and current are calculated at one minute
 231 intervals.

232 The SMT6 (60) P solar module manufactured by Romag, has been used in this work. The electrical
 233 characteristics of the solar module are shown in Table 1. The standard test condition (STC) for these solar
 234 panels are:

- 235 • Solar Irradiance = 1000 W/m²
- 236 • Module Temperature = 25 °C

237 The fault detection algorithm has been validated experimentally over a 5 day period. On each day a
 238 different fault was perturbed as shown in Fig. 8:

- 239 1. Day1: Normal operation mode and partial shading effects on the GCPV plant (no fault occurred
- 240 in any of the tested PV modules),
- 241 2. Day2: One faulty PV module and partial shading effects on the GCPV plant
- 242 3. Day3: Two faulty PV modules and partial shading effects on the GCPV plant
- 243 4. Day4: Three faulty PV modules and partial shading effects on the GCPV plant
- 244 5. Day5: Four faulty PV modules and partial shading effects on the GCPV plant

245 In order to test the effectiveness of the proposed fault detection algorithm, the theoretical and the
 246 measured output power for each case scenario was logged and compared using VI LabVIEW software.

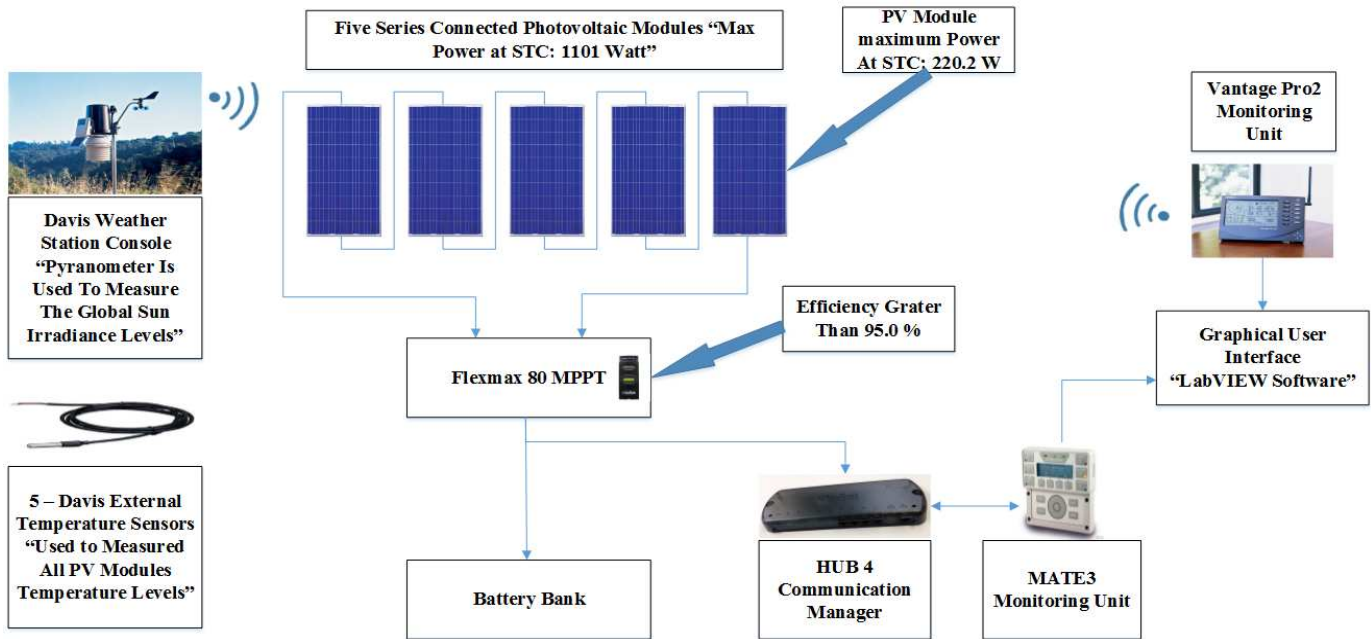


Fig. 7. Examined GCPV Plant Installed at the Huddersfield University, United Kingdom

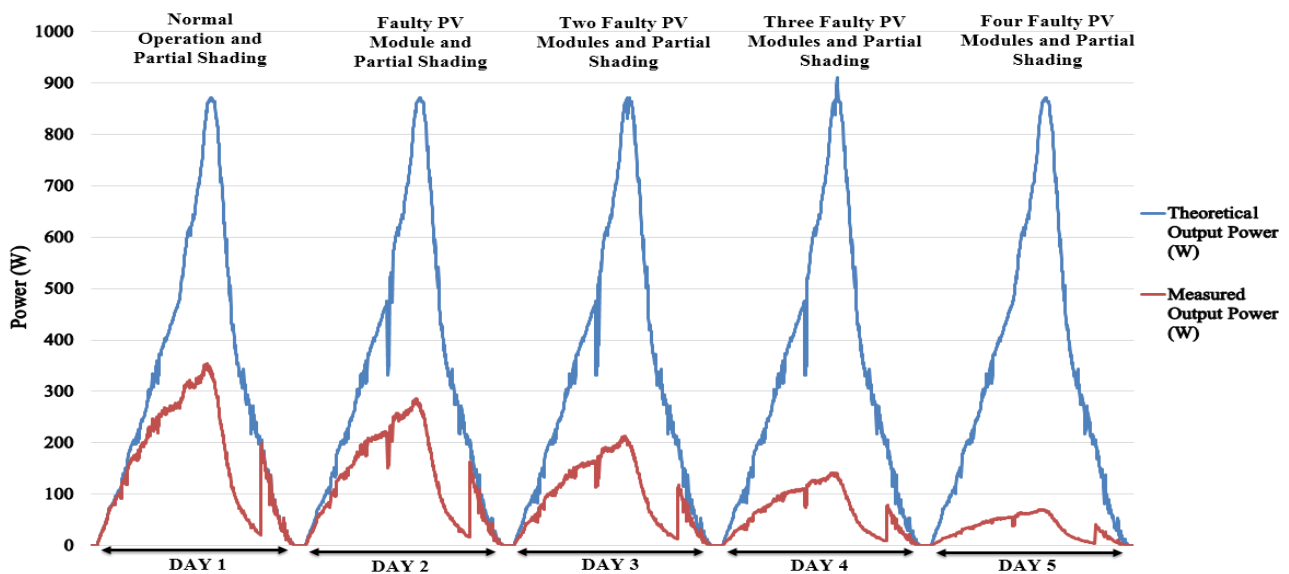


Fig. 8. Theoretical vs. Measured output power during 5 different days

247 **3.2 Evaluation of the Proposed Theoretical Curves Modelling**

248 In this section, the performance of the fault detection algorithm (theoretical curves modelling) is verified
 249 using normal operation mode and partial shading effects the GCPV system. Fig. 9 describes the
 250 theoretical simulation vs. the real-time long-term data measurement.

251 In order to apply a partial shading condition to the GPCV modules an opaque paper object has been used.
 252 The partial shading was applied to all PV modules at the same rate. Partial shading condition is increased
 253 during the test.

254 Fig. 10(A) shows the entire measured data vs. the theoretical detection limits which are discussed
 255 previously in section 2.2. As can be noticed, most of the measured data lies within the high and low
 256 theoretical detection limits which are created using 3rd order polynomial function. The high and low
 257 detection limit functions are also illustrated in the Fig 10(A).

258 The voltage ratio (VR) and power ratio (PR) for this particular test is shown in Fig 10(B). Since the PS
 259 condition applied to the GCPV system is increasing, therefore, both VR and PR ratios are increasing
 260 slightly during the test. Moreover, both ratios can be measured using (9). Fig. 10(B) shows the efficiency
 261 of the GCPV plant. The efficiency is evaluated using (10).

262
$$\text{Efficiency} = \frac{\text{Measured Output Power}}{\text{Theoretical Power}} \quad (10)$$

263 From Fig. 10(B), the efficiency of the GCPV system decreased while increasing the PS applied to the PV
 264 system. The detection accuracy (DA) for the proposed theoretical curves modelling algorithm can be
 265 expressed by (11).

266
$$\text{Detection accuracy (DA)} = \frac{\text{Total Number of Samples} - \text{Out of Region Samples}}{\text{Total Number of Samples}} \quad (11)$$

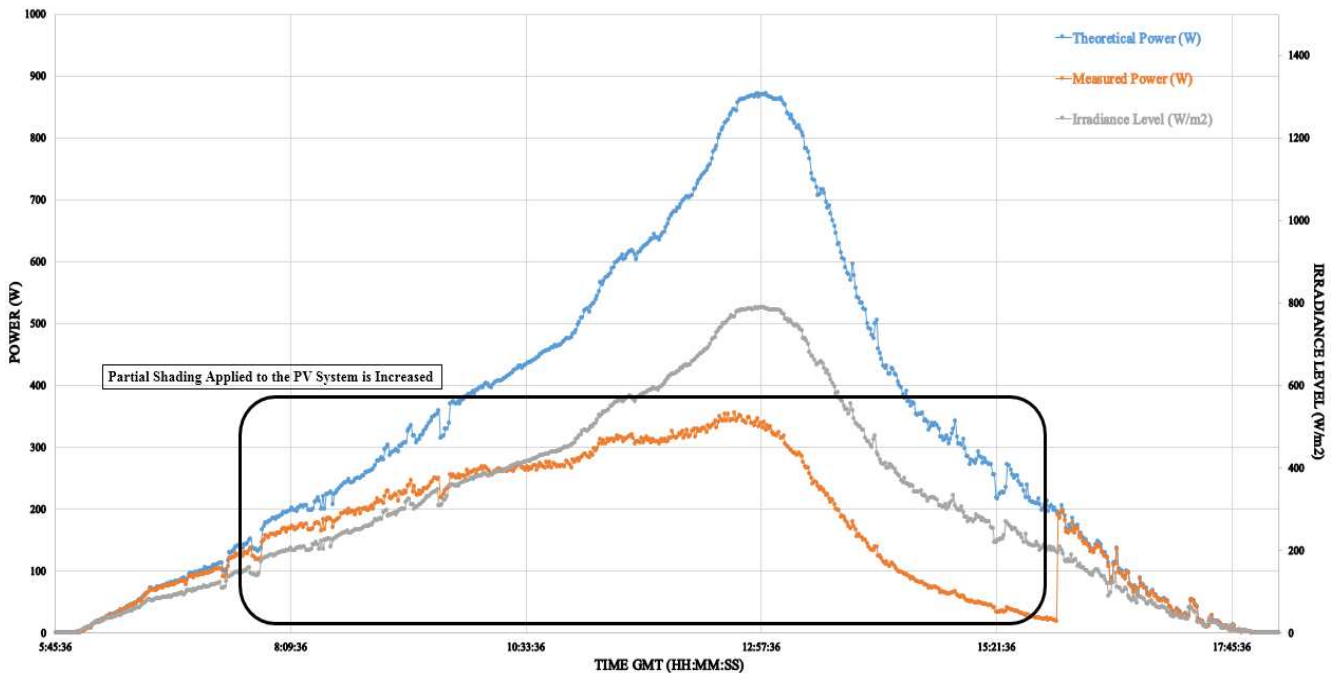


Fig. 9. Theoretical power vs. measured output power for a partial shading effects the GCPV plant

267 Using (11), the proposed algorithm has a detection accuracy equals to:

268
$$\text{Detection accuracy for the partial shading condtion} = \frac{720 - 37}{720} = 0.9486 = 94.86\%$$

269 In this test, the theoretical curves modelling fault detection algorithm shows a significant success for
 270 detecting partial shading conditions applied to the GCPV plant. The detection accuracy rate can be
 271 increased using a fuzzy logic classification system. Therefore, out of region samples (samples which are
 272 away from the high and low detection limits) are processed by the fuzzy logic system.

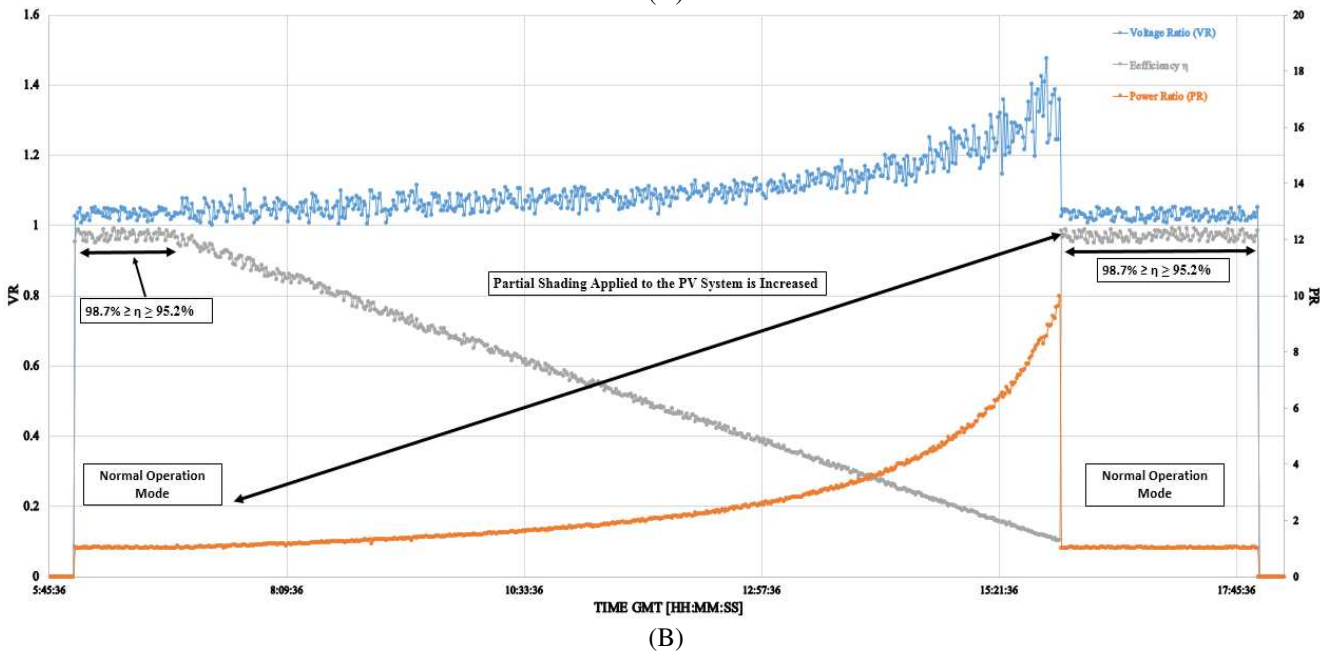
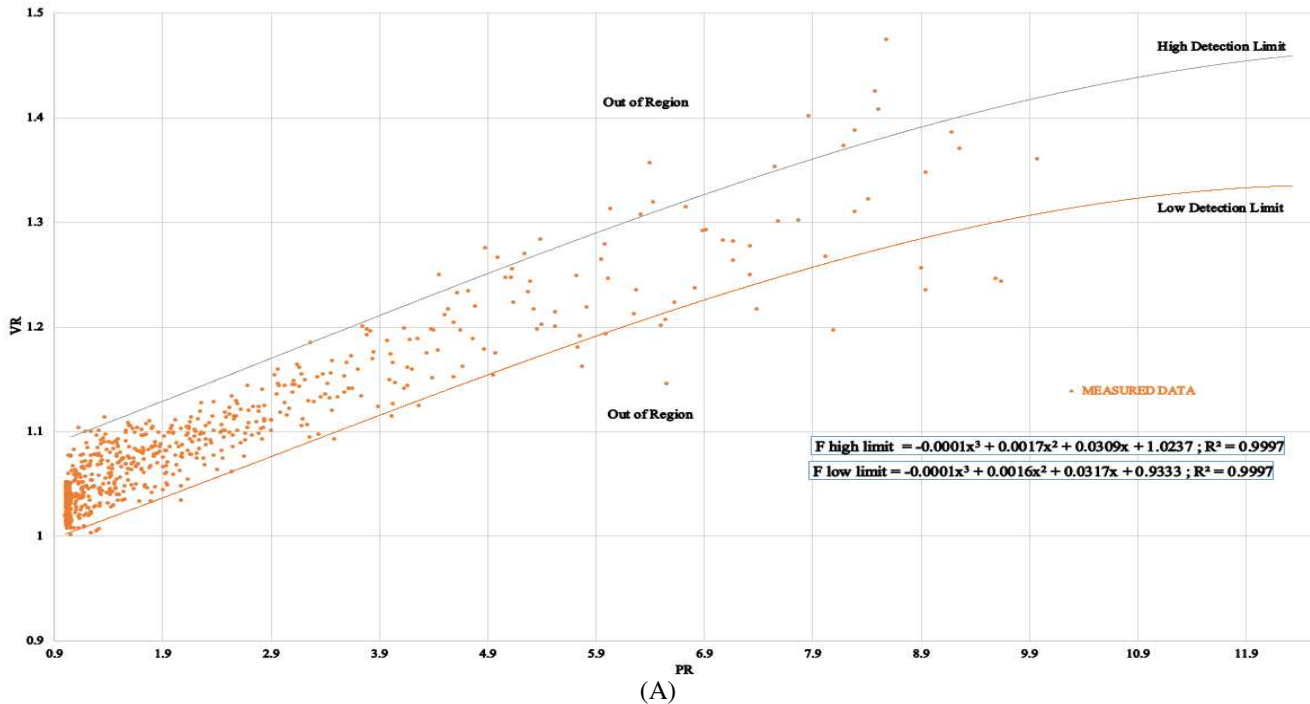


Fig. 10. Theoretical curves vs. real time long term measured data. (A) Theoretical fault curve detection limits for the examined GCPV plant, (B) Voltage ratio, power ratio and the efficiency of the entire GCPV system

273 **3.3 Evaluation of the Proposed Fuzzy Logic Classification System**

274 This test is created to confirm the ability of the fault detection algorithm to detect faulty PV modules
275 occurring in the GCPV plant using theoretical curves modelling algorithm and fuzzy logic classification
276 system. Four different case scenarios have been tested:

- 277 A. Faulty PV module with partial shading condition
- 278 B. Two faulty PV modules with partial shading condition
- 279 C. Three faulty PV modules with partial shading condition
- 280 D. Four faulty PV module and partial shading condition

281 Each case scenario is examined during a time period of a full day as shown Fig. 8 (Day 2, 3, 4 and 5),
282 where the total number of samples for each examined day are equal to 720 samples. Fig. 10 shows the
283 theoretical curve limits vs. real-time long-term measured data. 3rd order polynomial function of the
284 theoretical high and low limits is plotted, while the minimum determination factor (R) is equal to 99.59%.

285 As can be noticed, the measured data for each test is plotted and compared with the theoretical curve
286 limits. Most of the measured data among the 4 day test period lies within the high and low detection
287 limits of the theoretical curves. However, in each day, several out of region samples have been detected as
288 shown in Fig. 11.

289 The detection accuracy (DA) for each case scenario is calculated using (11) and reported in Table 2. The
290 minimum and maximum DA is equal to 94.03% and 95.27% respectively before considering the fuzzy
291 logic classification system.

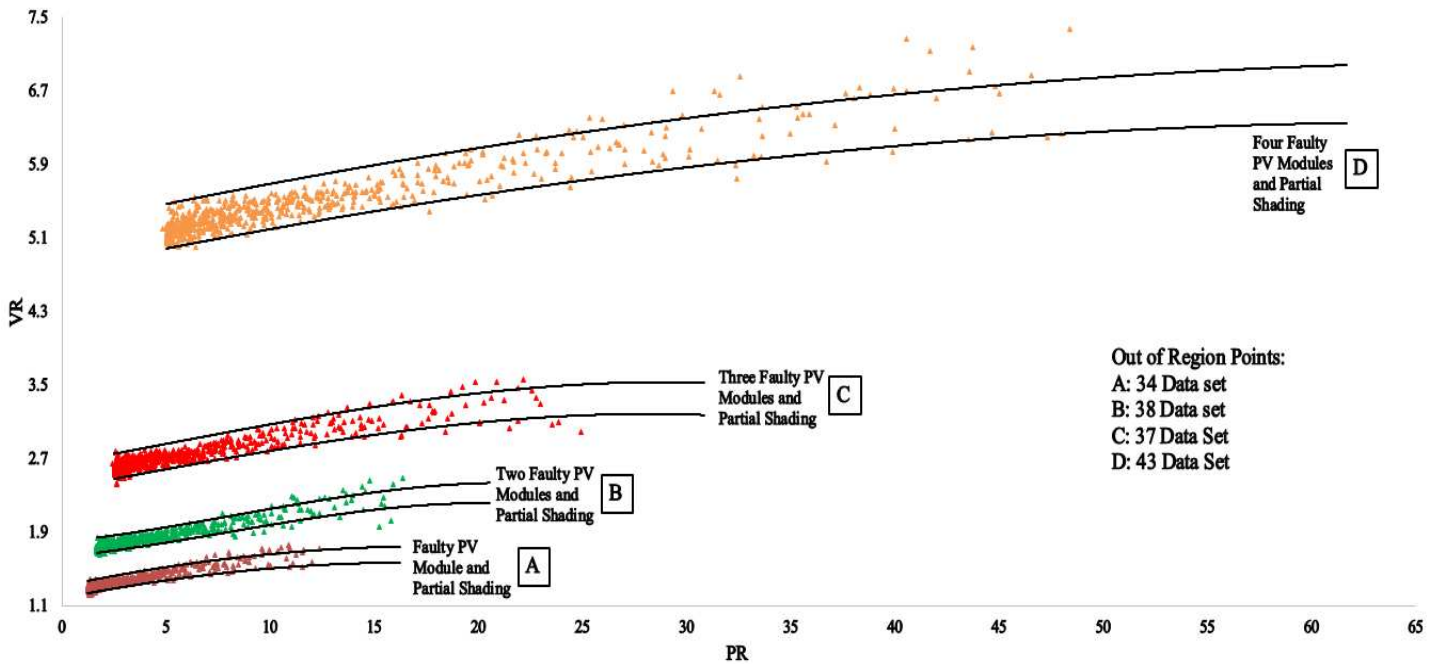


Fig. 11. Theoretical detection limits vs. real-time long-term data measurements for one faulty, two faulty, three faulty and four faulty photovoltaic modules

292 For each test including the test illustrated in section 3.2, out of region samples have been processed by the
 293 fuzzy logic classification system. Fig. 12 describes the performance of the fuzzy logic system during each
 294 test:

- 295 • Test 1: PS, described in section 3.2
- 296 • Test 2: One faulty PV module and PS
- 297 • Test 3: Two faulty PV modules and PS
- 298 • Test 4: Three faulty PV modules and PS
- 299 • Test 5: Four faulty PV modules and PS

300 It is evident that most of the samples are categorized correctly by the fuzzy classifier. For example, before
 301 considering the fuzzy logic system, the DA for test 2 is equal to 95.27% while the DA increased up to
 302 99.03% after taking into account the fuzzy logic classification system. This result is due to the detection
 303 of the out of region samples. The results for this test is shown in Fig. 12, only 7 out of 34 processed
 304 samples are detected incorrectly, while 27 samples have been detected correctly within an output
 305 membership function between 0.2 and 0.4.

306 Table 2 shows number of out of region samples and the detection accuracy (DA) for each test separately.
 307 The DA rate is increased up to a minimum value equals to 98.8%.

308 In this section, the evaluation for the theoretical curves modelling algorithm and the fuzzy logic system
 309 are discussed and briefly explained. From the obtained results, it is confirmed that the fault detection
 310 algorithm proposed in this article is suitable for detecting faulty conditions in PV systems accurately.

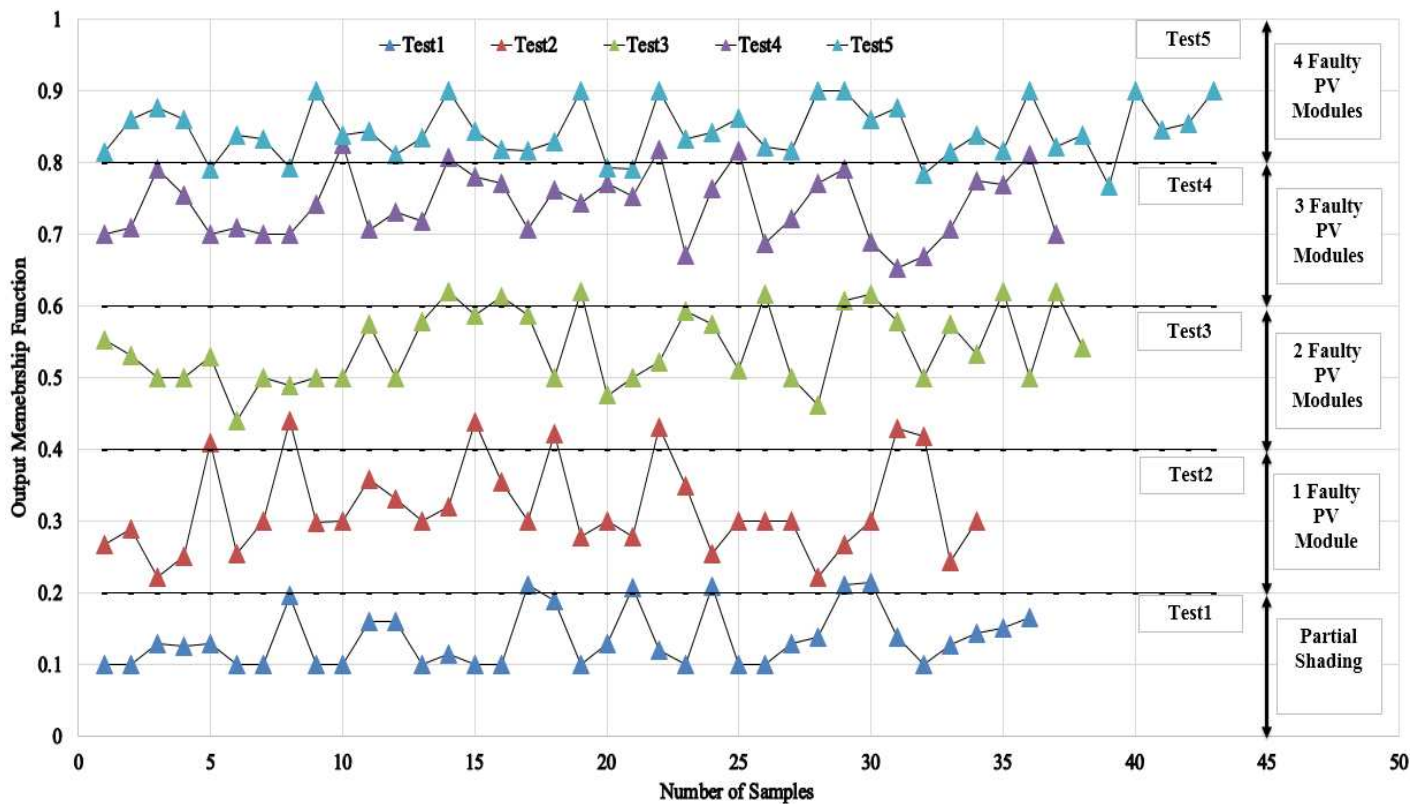


Fig. 12. Out of region samples processed by the fuzzy logic classification system

TABLE 2
EFFICIENCY COMPARISON BETWEEN FOUR DIFFERENT CASE SCENARIOS

Test Number	Case Scenario	Without Fuzzy Classifier		Including Fuzzy Classifier	
		Out of Region Samples	Detection Accuracy (DA %)	Out of Region Samples	Detection Accuracy (DA %)
Test 1 (described in section 3.2)	Partial shading effects the GCPV system	37	94.86	5	99.31
Test 2 (presented as A in Fig. 11)	Faulty PV module and partial shading	34	95.27	7	99.03
Test 3 (presented as B in Fig. 11)	Two faulty PV module and partial shading	38	94.72	8	98.80
Test 4 (presented as C in Fig. 11)	Three faulty PV module and partial shading	37	94.86	5	99.31
Test 5 (presented as D in Fig. 11)	Four faulty PV module and partial shading	43	94.03	6	99.16

3.4 Performance Evaluation of the Proposed Fault Detection Algorithm Based on Array Ages

Since the examined PV modules used in the previous sections is new (installed 2 years ago), the proposed PV detection algorithm was evaluated using another PV system as shows in Fig. 13, where the total PV system capacity is equal to 0.52 kWp. The MPPT unit is previously explained in section 3.1. The PV modules are installed at the University of Huddersfield 11 years ago.

Before considering the PV age of installation, the detection limits obtained using (4-7) shows low detection accuracy since the PV degradation rate is not considered. The results are shown in Fig. 14 for various tests, were the maximum detection accuracy is equal to 63.8%. Therefore, the formulas (6 & 7) are updated to contain the PV array degradation rate as described by (12 & 13).

$$PR \text{ Low limit} = \frac{P_{G,T}}{((P_{G,T} - nP_0) \eta_{sensor}) \times (100 - \text{Accumulative PV Degredation Rate})} \quad (12)$$

$$VR \text{ Low limit} = \frac{V_{G,T}}{((V_{G,T} - nV_0) \eta_{sensor1}) \times (100 - \text{Accumulative PV Degredation Rate})} \quad (13)$$

Where the accumulative PV degradation rate is calculated using (14).

$$\text{Accumulative PV Degredation Rate} = PV \text{ Degredation rate per year} \times PV \text{ Age of Instllation} \quad (14)$$

The value of the degradation rate per year in Huddersfield/UK has been calculated at a degradation rate equals to 0.67%/year. As a result, using (14) the accumulative degradation rate of the examined PV modules is equal to:

$$\text{Accumulative PV Degredation Rate} = 0.67 \left(\frac{\text{degredation}}{\text{year}} \right) \times 11 (PV \text{ Age of Instllation}) = 7.37$$

Various results have been conducted after evaluating the PV degradation rate of the existing PV system, the detection accuracy of the proposed fault detection limits is approximately equal to 94% comparing to 63.8% before considering the PV array age of installation as illustrated in Fig. 14. In order to increase the detection accuracy of the proposed fault detection limits, it is required to use the fuzzy logic system described in section 2.3.

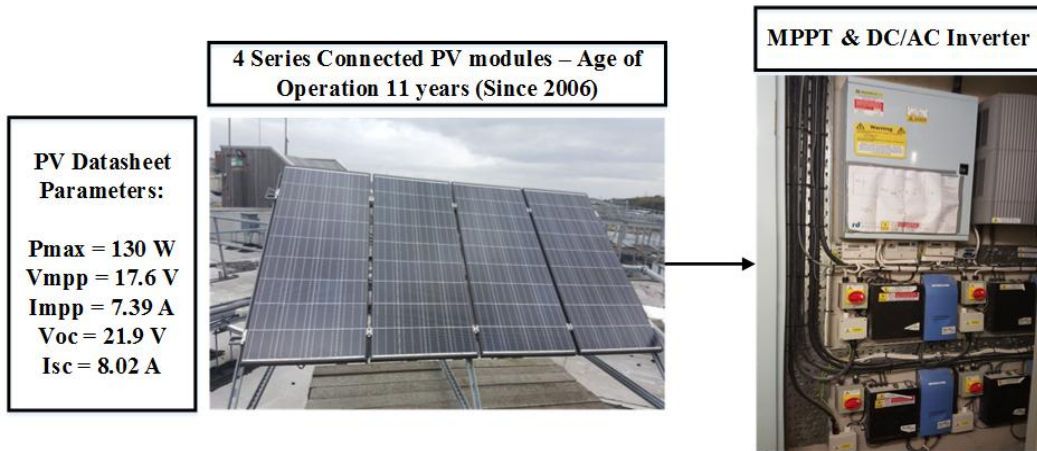


Fig. 13. Second examined PV system installed at the University of Huddersfield - year of installation: 2006

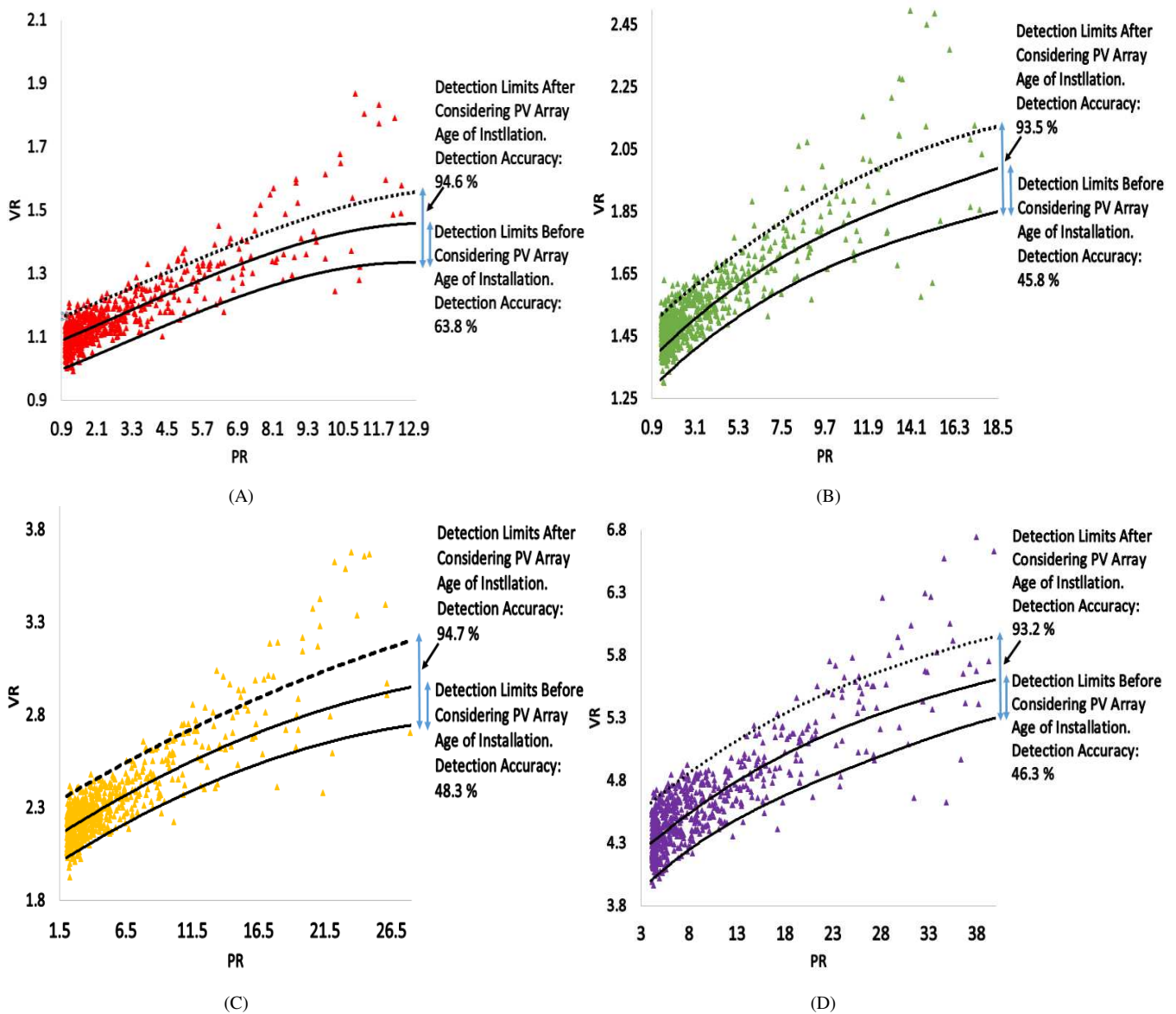


Fig. 14. Theoretical detection limits vs. real-time long-term data measurements before and after considering the age of the PV array.
 (A) Normal operation mode and partial shading, (B) One faulty PV module and partial shading, (C) Two faulty PV modules and Partial shading, (D) Three faulty PV modules and partial shading

333 **3.5 Discussion**

334 In order to test the effectiveness of the proposed fault detection algorithm presented in this paper, the
335 results obtained have been compared with multiple fault detection approaches. The common combination
336 between the proposed algorithm in this paper and the research demonstrated by [5, 8 and 26] is the VR
337 and PR equations. However, the VR and PR equations presented in this work have a different parameters
338 such as:

- 339 1. VR and PR equations contain the number of modules that are examined in the GCPV plant,
340 which is presented using the variable: n .
- 341 2. Both equations contain the voltage and current sensors uncertainly (sensor efficiency rate), which
342 makes the algorithm easier to use with different PV installations.
- 343 3. The detection limits (high and low) is a novel idea which has not been presented by any other
344 research article related to fault detection algorithms in PV systems.

345 Moreover, by using VR and PR ratios it was evident that the algorithm can detect up to $(n-1)$ faulty PV
346 modules and PS effects the GCPV plant, where n is equal to the number of PV modules in the examined
347 GCPV installation.

348 In [7 and 12] statistical analysis technique based on standard deviation limits are used to detect possible
349 faults in the GCPV plant, however, the presented techniques cannot identify the type of the fault occurred
350 in the PV system, therefore, it is necessary to create a new mathematical calculations of the entire GCPV
351 plant. In this paper, it is presented that the algorithm is based on the analysis of the theoretical curves
352 modelling using 3rd order polynomial functions, without the use of any statistical analysis approaches.

353 Furthermore, [10] experimented another tactical statistical analysis technique called t-test. This algorithm
354 is capable to detect multiple faults in PV systems, however, the ratios used to monitor the performance of
355 the PV system does not contain any parameter for the number of PV modules and the uncertainly in the
356 internal voltage and current sensors used.

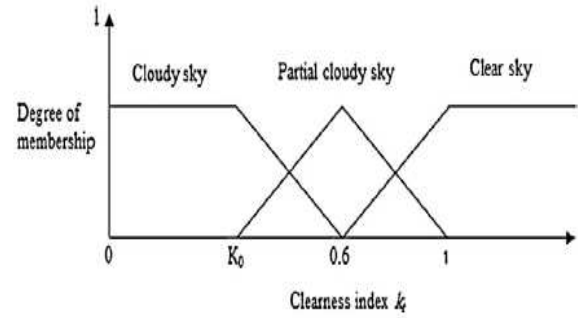
357 There are variety of fuzzy logic control systems used with PV applications. Three-phase three-level grid
358 interactive inverter with fuzzy based maximum power point tracking controller is presented by [27].
359 Additionally, some of the fuzzy logic classification systems were used with hybrid green power systems
360 as reported by S. Safari et al [28]. Furthermore, M. Tadj et al [5] presented a fuzzy logic technique which
361 is used to estimate the solar radiation, the proposed technique contains three membership functions:
362 cloudy sky, partial cloudy sky and clear sky. However, in this paper, a new attempt for using fuzzy logic
363 classification system to detect possible faults occurring in the PV plans. The main purpose of the fuzzy
364 logic presented in this work is to detect out of region samples (samples that lies away from the high and
365 low theoretical detection limits), and therefore, to increase the detection accuracy of the fault detection
366 algorithm. The fuzzy logic system can be reused with other GCPV plants by changing the parameters
367 which are shown in Fig. 5.

368 A comparison between the output membership functions developed by [5] and this study are shown in
369 Fig. 15(A) and Fig. 15(B) respectively. In [1] authors' used Mamdani fuzzy logic system for enhancing
370 the detection of partial shading conditions effecting the PV plant, where the proposed mathematical
371 calculations of the fuzzy logic system is also presented in Fig. 15(A). Moreover, the fuzzy logic system
372 presented in this paper is used to detect out of region samples that are not detected using the theoretical
373 detection limits. Where the maximum detection accuracy achieved using the fuzzy logic system is equal
374 to 99.31%.

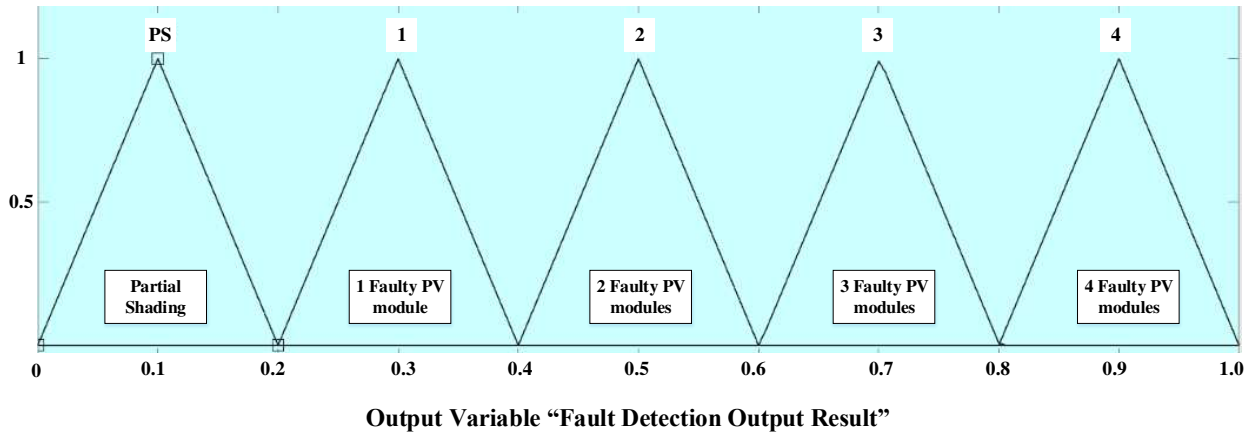
Clear sky : $Rib \leq Rc : k_t = 1$

Partially covered sky : $Rc < Rib < Rn : k_t = 1 - (1 - K_0) \frac{(Rib - Rc)}{(Rn - Rc)}$

Completely covered sky : $Rib \geq Rn : k_t = K_0$



(A)



(B)

Fig. 15. Fuzzy logic models. (A) Output membership functions proposed by M. Tadj [5], (B) Output membership functions suggested by this research

375 The fault detection algorithm presented in this work contains some advantages and disadvantages such as:

376 **Advantages:**

- 377 • The algorithm does not use a statistical analysis approach to detect possible faults in the GCPV
- 378 system. However, many recent article including [7, 10 and 12] depends on various statistical
- 379 techniques to detect faults in PV systems.
- 380 • The fault detection algorithm can be used with wide range of PV installation, since it depends on
- 381 the analysis of the power and the voltage ratios which are normally available in most GCPV
- 382 systems.
- 383 • Multiple faults can be detected accurately, the minimum and maximum detection accuracy
- 384 obtained by the algorithm are equal to 98.8% and 99.31% respectively.
- 385 • The efficiency of the voltage and current sensor has been taken into account in the mathematical
- 386 modelling for the proposed fault detection algorithm.
- 387 • The fuzzy logic classification system is easy to be reused in other PV systems since it depends
- 388 only on the analysis of the VR and PR.
- 389 • In order to include the PV age of installation degradation rate, VR and PR ratios have been
- 390 modified and analyzed using an old PV installation (age of PV plant is 11 years).

392 **Disadvantages:**

- 393 • The algorithm depends on the voltage and the power ratios of the GCPV systems. Therefore, the
- 394 accuracy of the algorithm depends on the instrumentation used in the PV plants.

- 395 • The algorithm is not capable of detecting faults occurring in the bypass diodes, which are
396 commonly used nowadays with PV systems. This problem in GCPV plants has been investigated
397 by W. Chine [9].
- 398 • The fault detection algorithm cannot detect any fault arising in the DC/AC inverter units which
399 are commonly used with GCPV systems. This type of fault has been reported by R. Platon et al
400 [12], G. Bayrak [21] and F. Deng et al [29].
- 401

402 4. **Conclusion**

403 In this work, a new GCPV fault detection algorithm is proposed. The developed fault detection algorithm
404 is capable of detecting faulty PV modules and partial shading conditions which affect GCPV systems.
405 The detection algorithm has been tested using 1.1kWp and 0.52kWp GCPV systems installed at
406 Huddersfield University, United Kingdom.

407 The fault detection algorithm consist of six layers working in series. The first layer contains the input
408 parameters of the sun irradiance and PV modules' temperature, while the second layer generates the
409 GCPV theoretical performance analysis using Virtual Instrumentation (VI) LabVIEW software. Layer 3
410 identifies the power and voltage ratios, subsequently creates a high and low detection limits which will be
411 used in Layer 4 to apply the 3rd order polynomial regression model on the top of the PR and VR ratios.
412 The fifth layer consists of two parts: the input parameters of the examined GCPV systems and the 3rd
413 order polynomial detection limits. If the measured voltage ratio vs. measured power ratio lies away from
414 the detection limits, the samples will be processed by the last layer which contains the fuzzy logic
415 classification system.

416 The novel contribution of this research is that the fault detection algorithm depends on the variations of
417 the voltage and the power of the GCPV plant. Additionally, there are a few fuzzy logic classification
418 systems which are used with PV fault detection algorithms, therefore, this research introduced a simple,
419 reliable and quick fuzzy logic classification system which can be used with various GCPV plants.

420 The results indicate that the fault detection algorithm is capable of detecting most of the measured data
421 within the theoretical limits created using 3rd order polynomial functions. Furthermore, the maximum
422 detection accuracy of the algorithm before considering the fuzzy logic system is equal to 95.27%,
423 however, the fault detection accuracy is increased up to a minimum value of 98.8% after considering the
424 fuzzy logic system.

425 5. **Acknowledgment**

426 The authors would like to acknowledge the financial support to the University of Huddersfield,
427 engineering and computing department.

428

429 **References**

- 430 [1] Monteiro, R. V., Guimarães, G. C., Moura, F. A., Albertini, M. R., & Albertini, M. K. (2017). Estimating
431 photovoltaic power generation: Performance analysis of artificial neural networks, Support Vector Machine
432 and Kalman filter. *Electric Power Systems Research*, 143, 643-656.

- 433 [2] Torres-Ramírez, M., Nofuentes, G., Silva, J. P., Silvestre, S., & Muñoz, J. V. (2014). Study on analytical
434 modelling approaches to the performance of thin film PV modules in sunny inland climates. *Energy*, 73,
435 731-740.
- 436 [3] Ruiz-Rodriguez, F. J., Hernandez, J. C., & Jurado, F. (2012). Probabilistic load flow for photovoltaic
437 distributed generation using the Cornish–Fisher expansion. *Electric Power Systems Research*, 89, 129-138.
- 438 [4] Alam, M. K., Khan, F., Johnson, J., & Flicker, J. (2015). A comprehensive review of catastrophic faults in
439 PV arrays: Types, detection, and mitigation techniques. *IEEE Journal of Photovoltaics*, 5(3), 982-997.
- 440 [5] Tadj, M., Benmouiza, K., Cheknane, A., & Silvestre, S. (2014). Improving the performance of PV systems
441 by faults detection using GISTEL approach. *Energy conversion and management*, 80, 298-304.
- 442 [6] Takashima, T., Yamaguchi, J., Otani, K., Oozeki, T., Kato, K., & Ishida, M. (2009). Experimental studies
443 of fault location in PV module strings. *Solar Energy Materials and Solar Cells*, 93(6), 1079-1082.
- 444 [7] Chouder, A., & Silvestre, S. (2010). Automatic supervision and fault detection of PV systems based on
445 power losses analysis. *Energy Conversion and Management*, 51(10), 1929-1937.
- 446 [8] Silvestre, S., Kichou, S., Chouder, A., Nofuentes, G., & Karatepe, E. (2015). Analysis of current and
447 voltage indicators in grid connected PV (photovoltaic) systems working in faulty and partial shading
448 conditions. *Energy*, 86, 42-50.
- 449 [9] Chine, W., Mellit, A., Lughi, V., Malek, A., Sulligoi, G., & Pavan, A. M. (2016). A novel fault diagnosis
450 technique for photovoltaic systems based on artificial neural networks. *Renewable Energy*, 90, 501-512.
- 451 [10] Dhimish, M., & Holmes, V. (2016). Fault detection algorithm for grid-connected photovoltaic plants. *Solar
452 Energy*, 137, 236-245.
- 453 [11] Dhimish, M., Holmes, V., & Dales, M. (2016, September). Grid-connected PV virtual instrument system
454 (GCPV-VIS) for detecting photovoltaic failure. In *Environment Friendly Energies and Applications
455 (EFEA), 2016 4th International Symposium on* (pp. 1-6). IEEE.
- 456 [12] Platon, R., Martel, J., Woodruff, N., & Chau, T. Y. (2015). Online Fault Detection in PV Systems. *IEEE
457 Transactions on Sustainable Energy*, 6(4), 1200-1207.
- 458 [13] Kim, K. A., Seo, G. S., Cho, B. H., & Krein, P. T. (2016). Photovoltaic Hot-Spot Detection for Solar Panel
459 Substrings Using AC Parameter Characterization. *IEEE Transactions on Power Electronics*, 31(2), 1121-
460 1130.
- 461 [14] Silvestre, S., Kichou, S., Chouder, A., Nofuentes, G., & Karatepe, E. (2015). Analysis of current and
462 voltage indicators in grid connected PV (photovoltaic) systems working in faulty and partial shading
463 conditions. *Energy*, 86, 42-50.
- 464 [15] Obi, M., & Bass, R. (2016). Trends and challenges of grid-connected photovoltaic systems—A
465 review. *Renewable and Sustainable Energy Reviews*, 58, 1082-1094.
- 466 [16] Alam, M. K., Khan, F., Johnson, J., & Flicker, J. (2015). A Comprehensive Review of Catastrophic Faults
467 in PV Arrays: Types, Detection, and Mitigation Techniques. *IEEE Journal of Photovoltaics*, 5(3), 982-997.
- 468 [17] Khamis, A., Shareef, H., Bizkevelci, E., & Khatib, T. (2013). A review of islanding detection techniques
469 for renewable distributed generation systems. *Renewable and sustainable energy reviews*, 28, 483-493.
- 470 [18] Boukenoui, R., Salhi, H., Bradai, R., & Mellit, A. (2016). A new intelligent MPPT method for stand-alone
471 photovoltaic systems operating under fast transient variations of shading patterns. *Solar Energy*, 124, 124-
472 142.

- 473 [19] Mutlag, A. H., Shareef, H., Mohamed, A., Hannan, M. A., & Abd Ali, J. (2014). An improved fuzzy logic
474 controller design for PV inverters utilizing differential search optimization. *International Journal of*
475 *Photoenergy*, 2014.
- 476 [20] Chen, J. L., Kuo, C. L., Chen, S. J., Kao, C. C., Zhan, T. S., Lin, C. H., & Chen, Y. S. (2016). DC-Side
477 Fault Detection for Photovoltaic Energy Conversion System Using Fractional-Order Dynamic-Error-based
478 Fuzzy Petri Net Integrated with Intelligent Meters. *IET Renewable Power Generation*.
- 479 [21] Chao, K. H., Ho, S. H., & Wang, M. H. (2008). Modeling and fault diagnosis of a photovoltaic
480 system. *Electric Power Systems Research*, 78(1), 97-105.
- 481 [22] Dhimish, M., Holmes, V., & Dales, M. (2016, September). Grid-connected PV virtual instrument system
482 (GCPV-VIS) for detecting photovoltaic failure. In *Environment Friendly Energies and Applications*
483 *(EFEA), 2016 4th International Symposium on* (pp. 1-6). IEEE.
- 484 [23] McEvoy, A., Castaner, L., Markvart, T., 2012. Solar Cells: Materials, Manufacture and Operation.
485 Academic Press.
- 486 [24] Sera, D., Teodorescu, R., & Rodriguez, P. (2007). PV panel model based on datasheet values. Paper
487 presented at the 2392-2396. doi:10.1109/ISIE.2007.4374981
- 488 [25] Suganthi, L., Iniyar, S., & Samuel, A. A. (2015). Applications of fuzzy logic in renewable energy systems–
489 a review. *Renewable and Sustainable Energy Reviews*, 48, 585-607.
- 490 [26] Chine, W., Mellit, A., Pavan, A. M., & Kalogirou, S. A. (2014). Fault detection method for grid-connected
491 photovoltaic plants. *Renewable Energy*, 66, 99-110.
- 492 [27] Altin, N., & Ozdemir, S. (2013). Three-phase three-level grid interactive inverter with fuzzy logic based
493 maximum power point tracking controller. *Energy Conversion and Management*, 69, 17-26.
- 494 [28] Safari, S., Ardehali, M. M., & Sirizi, M. J. (2013). Particle swarm optimization based fuzzy logic controller
495 for autonomous green power energy system with hydrogen storage. *Energy conversion and*
496 *management*, 65, 41-49.
- 497 [29] Deng, F., Chen, Z., Khan, M. R., & Zhu, R. (2015). Fault detection and localization method for modular
498 multilevel converters. *IEEE Transactions on Power Electronics*, 30(5), 2721-2732.